Electric-field modulation of perpendicular magnetic anisotropy and damping constant in MgO/Co/Pt trilayers

A. Sakoguchi(砂古口藍子)[1], D. Oshima(大島大輝)[2], S. Iwata(岩田聡)[3] and T. Kato (加藤剛志)[2]

[1]Department of Electronics, Nagoya University, Nagoya 464-8603, Japan
[2]Institute of Materials and Systems for Sustainability, Nagoya University, Nagoya, 464-8603, Japan
[3]Nagoya Industrial Science Research Institute, Nagoya 464-0819, Japan

Electric field modulations of the perpendicular magnetic anisotropy (PMA) and magnetization dynamics of MgO/Co/Pt trilayers were measured by time-resolved magneto-optical Kerr effect (TRMOKE). The anisotropy field estimated from the anomalous Hall effect applying a field along in-plane was confirmed to be modified by the electric field, which results in the PMA variation with electric field of –32 fJ/(V·m). The PMA variation was also confirmed from TRMOKE measurements, which was estimated to be –47 fJ/(V·m). From TRMOKE measurements, we also observed the reduction of the inverse of relaxation time $1/\tau$ of the magnetization precession with increasing the electric field. The $1/\tau$ was analyzed by assuming the contributions of effective Gilbert damping α_{eff}, anisotropy distribution, anisotropy angle distribution, and two magnon scattering, and we found α_{eff} decreased with increasing the electric field whose modulation was –0.0046 nm/V, corresponding to –13% per 1 V/nm. These results are similar to the electric field effect in (001)-orientated MgO/CoFeB/Ta trilayers (A. Okada *et al.*, Appl. Phys. Lett. 105, 052415 (2014)), however our finding indicates similar PMA and α modulations are found in MgO/Co/Pt trilayers having MgO(111)/fcc-Co interface.

***Index Terms*—Gilbert damping, Magnetic anisotropy, Electric field, MgO/Co/Pt**

I. Introduction

Voltage-torque switching has been attracted much attention as a writing method in magnetic random access memories (MRAM) with low power consumption. The writing energy in the voltage-torque switching is estimated to be 1 fJ/bit, which is about 1/500 of the switching energy for the conventional spin transfer torque (STT) switching. In the voltage-torque switching, the magnetization precession is triggered by the change of perpendicular magnetic anisotropy (PMA) by applying a voltage pulse, and the magnetization switching completes by half period of the magnetization precession [1]. Matsumoto *et al*. pointed out tunings of PMA and Gilbert damping are crucial to reduce the writing error in voltage-torque MRAM [2]. Thus, for the stable magnetization switching, the electric field dependence of PMA as well as magnetization dynamics are both important topics to be understood. Many studies on the voltage-induced modulation of PMA has been carried out [3]-[5], whereas there are only a few reports on the magnetization dynamics under the application of voltage [6]-[8]. Okada *et al*. reported Gilbert damping of MgO/CoFeB/Ta system is modulated by the application of gate voltage [6], while Sasaki *et al*. did not observe the significant change of Gilbert damping of MgO/CoFeB/Ta system with the applied electric field [7].

In this study, we measured the magnetization dynamics by using time-resolved magneto-optical Kerr effect (TRMOKE) under the application of the electric field in MgO/Co/Pt trilayers which have a high PMA, and estimated the electric field modulation of the PMA and Gilbert damping. Large electric field modulation of the magnetic properties is reported in the MgO/Co/Pt trilayers [9], [10] due to the variation of electron numbers in the thin Co layer. The Gilbert damping is known to be sensitive to the density of states at the Fermi energy [11], [12], and thus large electric field modulation of the Gilbert damping due to the variation of electron number is expected in the MgO/Co/Pt system. Gilmore *et al.* reported the Gilbert damping is dependent on the crystallographic orientation due to the anisotropic Fermi surface [12]. The MgO/Co/Pt trilayer will have MgO(111)/fcc-Co interface which is different from MgO(001)/bcc-CoFe interface in the previously reported MgO/CoFeB/Ta trilayers. Therefore, it is interesting to compare the electric field modulation of PMA and damping of the MgO/Co/Pt trilayer with those of the previously reported MgO/CoFeB/Ta trilayers.

II. Experimental Method

ITO(20)/MgO(10)/Co(t_{Co})/Pt(1.6)/Ta(10)/thermally oxidized Si substrate (thickness in nanometer) was prepared by an rf magnetron systems. Structure and hysteresis loops of the MgO/Co/Pt trilayers were characterized by X-ray diffraction and alternating gradient field magnetometer, respectively. To measure anomalous Hall effect under the application of electric field, the film was microfabricated in a Hall-bar structure and the 100 μm squared pillar was fabricated at the center of the Hall-bar, and the gate electrode of ITO (15 nm) was deposited on the pillar (see Fig. 1). The gate voltage was applied from –3 V to 3 V corresponding to the electric field from –0.3 V/nm to 0.3 V/nm. Hysteresis loop along film normal direction was obtained from anomalous Hall effect (AHE). AHE was also measured under in-plane magnetic field to estimate the anisotropy field. The in-plane

Manuscript received March 16, 2021; revised XX XX, XXXX and XX XX, XXXX; accepted XX XX, XXXX. Date of publication XX XX, XXXX; date of current version XX XX, XXXX. Corresponding author: T. Kato (e-mail: kato.takeshi@b.mbox.nagoya-u.ac.jp).
Color versions of one or more of the figures in this paper are available online at http://ieeexplore.ieee.org.
Digital Object Identifier (inserted by IEEE).

component of the magnetization M_{inp} was calculated by using the relation; $M_{inp}/M_s = \sin\{\cos^{-1}(R_H/R_{Hmax})\}$, where M_s is the saturation magnetization, and R_H and R_{Hmax} are Hall resistance and the maximum Hall resistance, respectively.

TRMOKE was measured by pump-probe method using high power fiber laser with a wavelength of λ =1040 nm, a pulse width of 500 fs and a repetition frequency of 100 kHz [13]-[15]. Pump beam with λ = 1040 nm was incident to the film surface to excite the magnetization precession, and the magnetization precession was monitored by Kerr rotation angle of reflected probe beam with λ = 520 nm. The external magnetic field H_{ext} in the range of 5-14 kOe was applied in the direction of 73 ° from the film normal. The angular frequency ω and relaxation time τ of the magnetization precession were extracted from the damped oscillation signals in TRMOKE. The H_{ext} dependence of ω and τ of the precession were fitted to estimate effective anisotropy field H_k^{eff}, g-factor and effective damping constant α_{eff}.

FIG. 1 HERE (Note white space above and below.)

III. Result and discussions

A. *Structural analysis*

Figure 2 shows XRD profile of MgO(10)/Co(1.6)/Pt(1.6) trilayer. Beside the peak from Si substrate (shown as * in the figure), ITO 222 and β-Ta 002 peaks are visible, and broad peak around $2\theta = 40^\circ$ is due to the overlapping of fcc-Pt 111 and MgO 111. No peaks are seen near MgO 200 ($2\theta = 43^\circ$) and Pt 200 ($2\theta = 46^\circ$), and thus the present MgO/Co/Pt trilayer is considered to have MgO(111)/fcc-Co interface.

FIG. 2 HERE (Note white space above and below.)

B. *Anomalous Hall effect*

The MgO(10)/Co(1.2)/Pt(1.6) trilayer exhibited large PMA, and the coercivity in perpendicular direction was 160 Oe, which were obtained from AHE loop applying a magnetic field along perpendicular to the film plane (not shown here). Figure 3 (a) shows the AHE of MgO(10)/Co(1.2)/Pt(1.6) trilayer applying in-plane magnetic field under the application of the gate voltage of ±1.5 V. The in-plane component of the magnetization M_{inp} was calculated from Fig. 3 (a), and the linear behavior of in-plane *M-H* loops was observed as shown in Fig. 3 (b). The slope of in-plane *M-H* loops increased by applying a positive electric field. By the linear fitting of M_{inp}, effective anisotropy field H_k^{eff} was estimated to be H_k^{eff} = 4220 Oe for the electric field of E = 0.15 V/nm and H_k^{eff} = 4350 Oe for E = –0.15 V/nm. The electric field dependence of H_k^{eff} is discussed later in Fig. 4.

FIG. 3 HERE (Note white space above and below.)

C. *TRMOKE*

Figure 4 (a) shows the typical magnetization dynamics of MgO(10)/Co(1.2)/Pt(1.6) trilayer under the application of the gate voltage of ±3.0 V. In Fig. 4 (a) exponentially decayed background in the raw TRMOKE data was subtracted [13]. The external magnetic field of $\underline{H}_{ext}$ = 14 kOe was applied during the measurements. From Fig. 4 (a), both angular frequency ω and the relaxation time τ of the magnetization precession were confirmed to vary with the electric field. The effective anisotropy field H_k^{eff} was estimated from the following analytical expressions derived from Landau-Lifshitz-Gilbert equation [16], [17].

$$\begin{aligned}
&\omega = \gamma\sqrt{H_{X0}H_{Y0}},\\
&H_{X0} = H_{\text{ext}}\cos(\theta_{\text{H}}-\theta) + H_{\text{k}}^{\text{eff}}\cos^2\theta,\\
&H_{Y0} = H_{\text{ext}}\cos(\theta_{\text{H}}-\theta) + H_{\text{k}}^{\text{eff}}\cos 2\theta,
\end{aligned} \tag{1}$$

where $\gamma = \mu_B g/\hbar$ =1.105×10^5 g (m/A·s) is the gyromagnetic constant, θ_H is the direction of $\underline{H}_{ext}$ from the film normal, and θ is the stable magnetization angle from the film normal calculated by minimizing the following magnetic energy,

$$E = -M_{\text{s}}H_{\text{ext}}\cos(\theta_{\text{H}}-\theta) + \frac{M_{\text{s}}H_{\text{k}}^{\text{eff}}}{2}\sin^2\theta. \tag{2}$$

Figure 4 (b) is the electric field dependence of H_k^{eff} of the MgO(10)/Co(1.2)/Pt(1.6) trilayer estimated from TRMOKE. H_k^{eff} estimated from AHE was also shown as a comparison. There are some difference (roughly 10%) in the absolute value of H_k^{eff} between TRMOKE and AHE. This difference is considered to be due to the limited maximum field applied in AHE experiments (see Fig. 3). The electric field dependence of H_k^{eff} is similar in TRMOKE and AHE; H_k^{eff} decreased with increasing the electric field. The variation of PMA with electric field estimated from TRMOKE and AHE was –47 fJ/(V·m) and –32 fJ/(V·m), respectively.

FIG. 4 HERE (Note white space above and below.)

Figure 5 (a) shows the electric field dependence of the inverse of the relaxation time $1/\tau$ at H_{ext} = 14 kOe estimated from TRMOKE. Just as H_k^{eff}, $1/\tau$ also exhibited significant electric field dependence. Figure 5 (b) shows the magnetic field dependence of $1/\tau$ of MgO(10)/Co(1.2)/Pt(1.6) trilayer under E = 0.3 V/nm. Since $1/\tau$ is known to include Gilbert damping as well as the extrinsic contributions, such as anisotropy distribution and two magnon scattering (TMS) [17], the external field dependence of $1/\tau$ shown as closed circles in Fig. 5 (b) was fitted by assuming four contributions; effective Gilbert damping α_{eff}, anisotropy axis distribution $\Delta\theta_H$, anisotropy distribution ΔH_k^{eff} and two magnon scattering (TMS) [17]-[21].

$$\begin{aligned}
\frac{1}{\tau} &= \frac{1}{\tau_{\text{Gilbert}}} + \frac{1}{\tau_{\Delta\theta_{\text{H}}}} + \frac{1}{\tau_{\Delta H_{\text{k}}^{\text{eff}}}} + \frac{1}{\tau_{\text{TMS}}}\\
&= \alpha_{\text{eff}}\omega + \frac{1}{2}\left|\frac{\partial\omega}{\partial\theta_{\text{H}}}\right|\Delta\theta_{\text{H}} + \frac{1}{2}\left|\frac{\partial\omega}{\partial H_{\text{k}}^{\text{eff}}}\right|\Delta H_{\text{k}}^{\text{eff}}
\end{aligned}$$

$$+N_0 \sum_{\mathbf{k}} \frac{C(k)}{\omega} \mathrm{Im}\left(\frac{1}{\omega_{\mathbf{k}}^2 - \omega^2 + i\omega\delta\omega_{\mathbf{k}}}\right), \tag{3}$$

where N_0, $C(k)$, ω_k and $\delta\omega_k$ are the intensity of two magnon scattering, the correlation function, spin wave dispersion and inverse life time of the spin wave, respectively. Here, it was assumed that only H_k^{eff} and α_{eff} depend on the electric field to reproduce the experimental results. ΔH_k^{eff} and $1/\tau_{TMS}$ depend on H_k^{eff} and thus they depend on the electric field through the variation of H_k^{eff}. Details of the fitting are described in Appendix.

FIG. 5 HERE (Note white space above and below.)

Figure 6 (a) shows the electric field dependence of four constituents in (3) at H_{ext} = 14 kOe. Two contributions, effective damping α_{eff} and the extrinsic term of $\Delta\theta_H$, were found to be dominant on the relaxation of the precession, and these terms decreased with increasing the electric field. Thus, it is concluded that the electric field dependence of $1/\tau$ results from the sum of the electric field modulation of these two contributions. Figure 6 (b) shows the electric field dependence of α_{eff}, and the α_{eff} value decreased with increasing electric field with a ratio of –0.0046 nm/V, corresponding to –13 % per 1 V/nm. Okada *et al*., reported that damping constant α of MgO/CoFeB/Ta trilayers decreased linearly with increasing electric field [6]. The ratio of α modulation with the electric field was –0.003 nm/V, corresponding to –21 % per 1 V/nm. They also reported the decrease of PMA with increasing electric field with the variation of –60 fJ/(V·m). These results are similar to the results obtained in this study. Electric field modulation of the magnetic properties of metallic thin films is considered to originate from the variation of the electronic structure with a thickness of ~0.1 nm from the interface due to short Thomas-Fermi screening length in metal. MgO/Co/Pt trilayer in this study has MgO(111)/fcc-Co interface as shown in Fig. 1, and we expected different electric field modulation of α from that of previously reported MgO/CoFeB/Ta trilayers with MgO(001)/bcc-CoFe interface. In fact, the sign of the modulation of PMA was reported to depend on the underlayer [22], [23]. However, our results show that similar electric field dependence of PMA and α between (111)-oriented MgO/Co/Pt trilayer and (001)-oriented MgO/CoFeB/Ta trilayer.

FIG. 6 HERE (Note white space above and below.)

IV. SUMMARY

Electric field modulations of PMA and the Gilbert damping constant in MgO/Co/Pt trilayers have been investigated by means of TRMOKE and AHE. It was confirmed in both measurements that PMA decreased with increasing electric field where the variation of PMA was –47 fJ/(V·m) for TRMOKE and –32 fJ/(V·m) for AHE. The inverse of the relaxation time of magnetization precession, $1/\tau$ was also confirmed to be modified by the electric field. Effective damping constant α_{eff} was estimated from the H_{ext} dependence of $1/\tau$ under the application of the electric field from –0.3 V/nm to 0.3 V/nm. By considering four contributions to $1/\tau$; effective damping α_{eff}, anisotropy axis distribution $\Delta\theta_H$, anisotropy distribution ΔH_k^{eff}, and TMS, the contributions of α_{eff} and $\Delta\theta_H$ were found to be dominant. Both α_{eff} and $\Delta\theta_H$ terms decreased with increasing electric field, which is responsible for the electric field modulation of $1/\tau$. In the MgO/Co/Pt trilayer, α_{eff} was found to decrease with increasing electric field with a ratio of –0.0046 nm/V, corresponding to –13 % per 1 V/nm. The modulation of α_{eff} is comparable to that in previously reported MgO/CoFeB/Ta trilayers. The MgO/CoFeB/Ta trilayers are expected to have MgO(001)/bcc-CoFe interface, which is different structure from our MgO/Co/Pt with MgO(111)/fcc-Co interface. It was found a similar PMA and α modulations between (111)-orientated MgO/Co/Pt trilayers and (001)-orientated MgO/CoFeB/Ta trilayers.

APPENDIX

The external field dependence of the inverse of the relaxation time $1/\tau$ of the MgO/Co/Pt trilayer under various electric fields was fitted with (3). There were assumed to be four contributions to $1/\tau$; α_{eff}, $\Delta\theta_H$, ΔH_k^{eff} and TMS terms in (3). The TMS term is proportional to the scattering intensity N_0 which given by

$$N_0 = \gamma^4\big(4H_{X0}^2\cos^4\theta + 4H_{Y0}^2\cos^2 2\theta - 8H_{X0}H_{Y0}\cos^2\theta\cos 2\theta\big)(\Delta H_{\mathrm{k}}^{\mathrm{eff}})^2, \tag{4}$$

Spin wave dispersion $\omega_{\mathbf{k}}$ and inverse life time of the spin wave $\delta\omega_{\mathbf{k}}$ are expressed as

$$\omega_{\mathbf{k}} = \gamma\sqrt{H_X(\mathbf{k})H_Y(\mathbf{k})}, \tag{5}$$

$$\delta\omega_{\mathbf{k}} = \alpha_{\mathrm{eff}}\gamma\left(H_X(\mathbf{k}) + H_Y(\mathbf{k})\right), \tag{6}$$

and $H_X(\mathbf{k})$ and $H_Y(\mathbf{k})$ are expressed as

$$H_X(\mathbf{k}) = H_{X0} + \frac{M_s}{\mu_0}(1-N_k)\cos^2\phi_{\mathbf{k}} + \frac{2A_{ex}}{M_s}k^2,$$
$$H_Y(\mathbf{k}) = H_{Y0} + \frac{M_s}{\mu_0}(1-N_k) \times\Big\{-\sin^2\theta + \cos^2\theta\sin^2\phi_{\mathbf{k}}\Big\} + \frac{2A_{ex}}{M_s}k^2, \tag{7}$$

where, μ_0 is the permeability of vacuum, $\varphi_{\mathbf{k}}$ is the azimuth angle of the spin wave, A_{ex} is the exchange stiffness and N_k is wave number dependent demagnetization factor, which is expressed as

$$N_k = \frac{1 - e^{kt_{\mathrm{Co}}}}{kt_{\mathrm{Co}}}, \tag{8}$$

where t_{Co} is the thickness of Co layer. Correlation function

$C(k)$ is given by

$$C(k) = \frac{2\pi\xi^2}{\left(1+(k\xi)^2\right)^{3/2}}, \tag{9}$$

where ξ is the correlation length. In this study, we fixed the parameters to simplify the fitting as $\Delta\theta_H$ = 3.6 °, M_s = 1400 emu/cc, ξ = 5 nm, A_{ex} = 26 pJ/m, since these parameters are considered to be independent of applied electric field. ΔH_k^{eff} was assumed to be varied with PMA, and set to be 0.8% of perpendicular anisotropy field as,

$$\Delta H_k^{eff} = 0.008\left(H_k^{eff} + \frac{M_s}{\mu_0}\right). \tag{10}$$

H_k^{eff} under the electric field was taken from Fig. 3 (b).

Acknowledgment

The authors would like to thank M. Kumazawa of Nagoya University for assistance in the experiments. This work was supported in part by JSPS KAKENHI Grant Number (16H04328, 17H03249, 17K18878, 17K19068, 20H02182), TATEMATSU foundation, and Tanaka Kikinzoku Memorial Foundation. This work was also supported in part by the Project of Creation of Life Innovation Materials for Interdisciplinary and International Researcher Development of the Ministry of Education, Culture, Sports, Science and Technology (MEXT), Japan. A part of this work was performed under the Research Program of “Dynamic Alliance for Open Innovation Bridging Human, Environment and Materials” in “Network Joint Research Center for Materials and Devices.” A part of this work was conducted at the Nagoya University Nanofabrication Platform, supported by "Nanotechnology Platform Program” of MEXT, Japan.

References

[1] Y. Shiota, T. Nozaki, F. Bonell, S. Murakami, T. Shinjo, and Y. Suzuki, “Induction of coherent magnetization switching in a few atomic layers of FeCo using voltage pulses,” *Nat. Mater.,* vol. 11, pp. 39, 2012.

[2] R. Matsumoto, T. Sato, and H. Imamura, “Voltage-induced switching with long tolerance of voltage-pulse duration in a perpendicularly magnetized free layer,” *Appl. Phys. Exp.,* vol. 12, pp. 053003, 2019.

[3] Y. Kato, H. Yoda, Y. Saito, S. Oikawa, K. Fujii, M. Yoshiki, K. Koi, H. Sugiyama, M. Ishikawa, T. Inokuchi, N. Shimomura, M. Shimizu, S. Shirotori, B. Altansargai, Y. Ohsawa, K. Ikegami, A. Tiwari, and A. Kurobe, “Giant voltage-controlled magnetic anisotropy effect in a crystallographically strained CoFe system,” *Appl. Phys. Exp.*, vol.11, pp.053007, 2018

[4] C. G. Duan, J. P. Velev, R. F. Sabirianov, Z. Zhu, J. Chu, S. S. Jaswal, and E. Y. Tsymbal, “Surface Magnetoelectric Effect in Ferromagnetic Metal Films,” *Phys. Rev. Lett.,* vol. 101, pp. 137201, 2018.

[5] C. Bi, Y. Liu, T. Newhouse-lllige, M. Xu, M. Rosales, J. W. Freeland, O. Mryasov, S. Zhang, S. G. E. te Velthuis, and W. G. Wang, “Reversible Control of Co Magnetism by Voltage-Induced Oxidation,” *Phys. Rev. Lett.,* vol. 113, pp. 267202, 2014.

[6] A. Okada, K. Kanai, M. Yamonouchi, S. Ikeda, F. Matsukawa, and H. Ohno, “Electric-field effects on magnetic anisotropy and damping constant in Ta/CoFeB/MgO investigated by ferromagnetic resonance,” *Appl. Phys. Lett.,* vol. 105, pp. 052415, 2014.

[7] Y. Sasaki, K. Suzuki, A. Sugihara, A. Kamimaki, S. Iihama, Y. Ando, and S. Mizukami, “All-optical detection of magnetization precession in tunnel junctions under applied voltage,” *Appl. Phys. Exp.,* vol. 10, pp. 023002, 2017.

[8] B. Rana, C. A. Akosa, K, Miura, H. Takahashi, G. Tatara, and Y. Otani, “Nonliner Control of Damping Constant by Electric Field in Ultrathin Ferromagnetic Films,” *Phys. Rev. Appl.,* vol. 14, pp. 014037, 2020.

[9] D. Chiba, S. Fukami, K. Shimamura, N. Ishiwata, K. Kobayashi, and T. Ono, "Electrical control of the ferromagnetic phase transition in cobalt at room temperature", *Nat. Mater.*, vol. 10, pp. 853-856 (2011).

[10] K. Yamada, H. Kakizaki, K. Shimamura, M. Kawaguchi, S. Fukami, N. Ishiwata, D. Chiba, and T. Ono, "Electric field modulation of magnetic anisotropy in MgO/Co/Pt structure", *Appl. Phys. Express*, vol. 6, pp. 073004 (2013).

[11] V. Kambersky, "Spin-orbital Gilbert damping in common magnetic metals", *Phys. Rev. B*, vol. 76, pp. 134416 (2007).

[12] K. Gilmore, M. D. Stiles, J. Seib, D. Steiauf, and M. Fähnle, "Anisotropic damping of the magnetization dynamics in Ni, Co, and Fe", *Phys. Rev. B*, vol. 81, pp. 174414 (2010).

[13] T. Kato, K. Nakazawa, R. Komiya, S. Tsunashima, and S. Iwata, “Compositional Dependence of g-Factor and Damping Constant of GdFeCo Amorphous Alloy Films,” *IEEE Trans. Magn.,* vol. 44, no.11, pp. 3380-3383, Nov. 2008.

[14] T. Kato, Y. Matsumoto, S. Okamoto, N. Kikuchi, O. Kitakami, N. Nishizawa, S. Tsunashima, and S. Iwata, “Time-Resolved Magnetization Dynamics and Damping Constant of Sputtered Co/Ni Multilayers,” *IEEE Trans. Magn.,* vol. 47, no.10, pp. 3036-3039, Oct. 2011.

[15] T. Kato, Y. Matsumoto, S. Kashima, S. Okamoto, N. Kikuchi, S. Iwata, O. Kitakami, and S. Tsunashima, “Perpendicular Anisotropy and Gilbert Damping in Sputtered Co/Pd Multilayers,” *IEEE Trans. Magn.,* vol. 48, no.11, pp. 3288-3291, Nov. 2012.

[16] H. Suhl, “Ferromagnetic Resonance in Nickel Ferrite Between One and Two Kilomegacycles,” *Phys. Rev.,* vol. 97, pp. 555, 1955.

[17] J.-M. Beaujour, D. Ravelosona, I. Tudosa, E. E. Fullerton, and A. D. Kent, “Ferromagnetic resonance linewidth in ultrathin films with perpendicular magnetic anisotropy,” *Phys. Rev. B.,* vol. 80, pp. 180415(R), 2009.

[18] R. D. McMichael and P. Krivosik, “Classical model of extrinsic ferromagnetic resonance linewidth in ultrathin films,” *IEEE Trans. Magn.,* vol. 40, no. 1, pp. 2-11, Jan. 2004.

[19] P. Landeros, R. E. Arias, and D. L. Mills, “Two magnon scattering in ultrathin ferromagnets: The case where the magnetization is out of plane,” *Phys. Rev. B.,* vol. 77, pp. 214405, 2008.

[20] S. Iihama, A. Sakuma, H. Naganuma, M. Oogane, S. Mizukami, and Y. Ando, “Influence of $L1_0$ order parameter on Gilbert damping constants for FePd thin films investigated by means of time-resolved magneto-optical Kerr effect,” *Phys. Rev. B.,* vol. 94, pp. 174425, 2016.

[21] T. Kato, D. Oshima, and S. Iwata, “Ion irradiation for planar patterning of magnetic materials,” *Crystals*, vol. 9, pp. 27, 2019.

[22] Y. Shiota, F. Bonell, S. Miwa, N. Mizuochi, T. Shinjo, and Y. Suzuki, “Opposite signs of voltage-induced perpendicular magnetic anisotropy change in CoFeB/MgO junctions with different underlayers,” *Appl. Phys. Lett.*, vol. 103, pp. 082410, 2013.

[23] M. Zeng, J. Lourembam, and S. T. Lim, “Electric-field effect on magnetic anisotropy of MgO/CoFe/capping structures,” *J. Appl. Phys.*, vol. 126, pp. 153902, 2019.

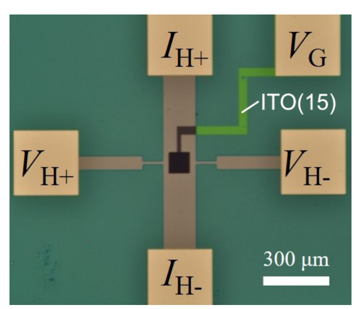

Fig. 1. Top view of a microfabricated MgO/Co/Pt device taken by optical microscope. $I_{H\pm}$ and $V_{H\pm}$ indicate the current and voltage terminals for the measurement of anomalous Hall effect, respectively, and V_G is the terminal for applying the gate voltage.

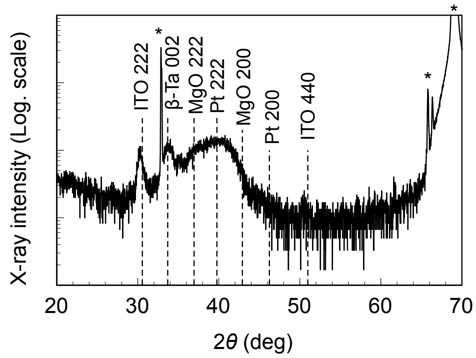

Fig. 2. XRD profile of ITO(20)/MgO(10)/Co(1.6)/Pt(1.6)/Ta(10)/substrate. The peaks indicated by * are from the Si substrate.

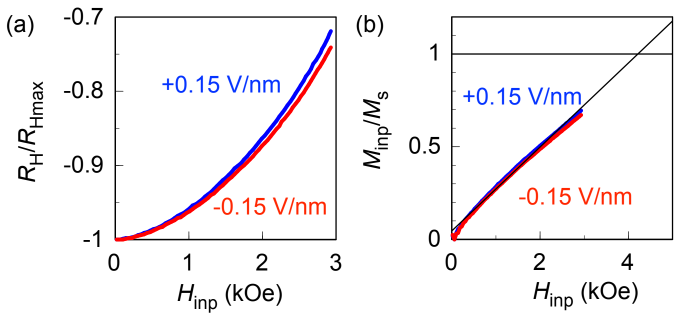

Fig. 3. (a) Normalized AHE of MgO(10)/Co(1.2)/Pt(1.6) trilayer taken applying in-plane magnetic field H_{inp} under the application of electric field E = 0.15 V/nm and –0.15 V/nm. (b) Normalized in-plane component of magnetization M_{inp}/M_s.

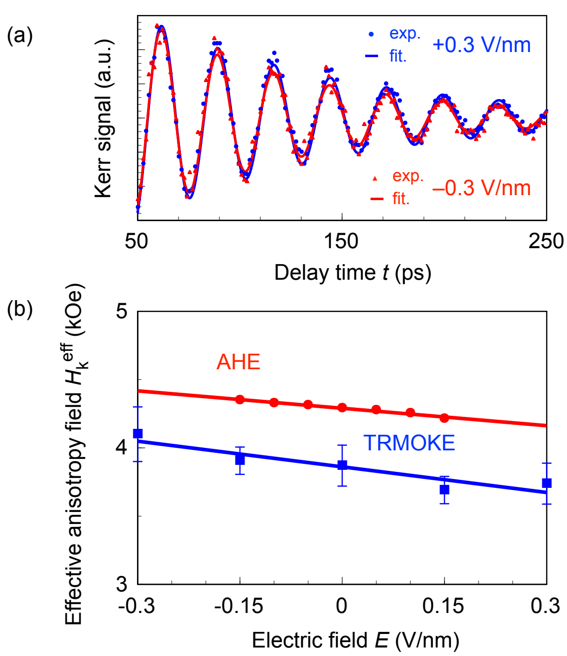

Fig. 4. (a) Magnetization dynamics of MgO(10)/Co(1.2)/Pt(1.6) trilayer obtained from TRMOKE measurements under the application of electric field E = 0.3 V/nm and –0.3 V/nm. (b) Electric field dependence of the effective anisotropy field H_k^{eff} of the MgO/Co/Pt trilayer obtained by TRMOKE and AHE.

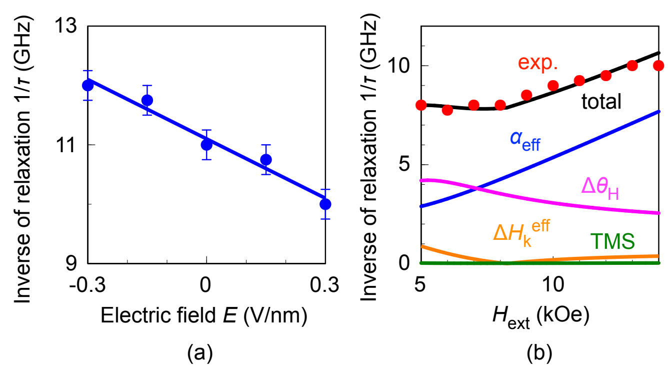

Fig. 5. (a) Electric field dependence of inverse of relaxation time $1/\tau$ of MgO(10)/Co(1.2)/Pt(1.6) trilayer at an external magnetic field H_{ext} = 14 kOe. (b) H_{ext} dependence of the inverse of relaxation time $1/\tau$ of the MgO/Co/Pt trilayer under the electric field of E = 0.3 V/nm. The closed circles show the experimental results, which were fit by assuming that $1/\tau$ consists of four contributions; effective Gilbert damping α_{eff}, anisotropy axis distribution $\Delta\theta_H$, anisotropy distribution ΔH_k^{eff} and two-magnon scattering (TMS). Each contribution and the sum of these contributions are also shown as solid lines in the figure.

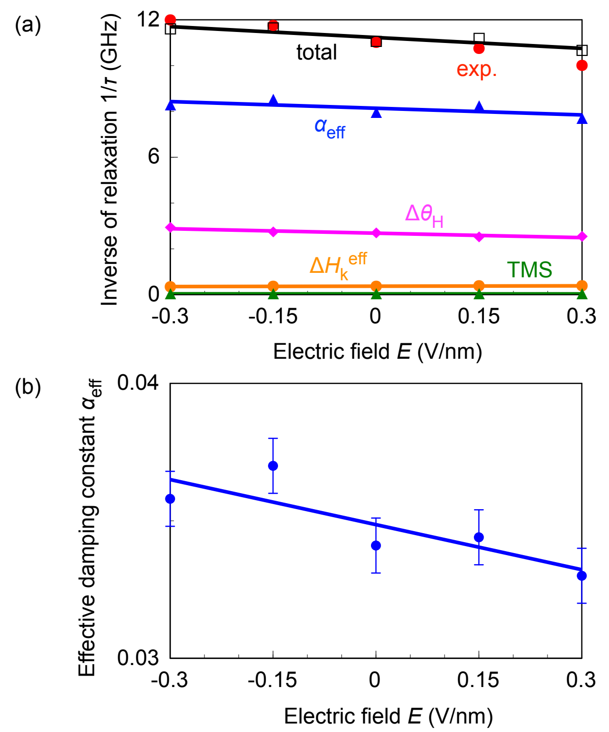

Fig. 6. (a) Electric field dependence of inverse of relaxation time at external magnetic field H_{ext} = 14 kOe. Experimental values of the inverse of relaxation time $1/\tau$ of MgO(10)/Co(1.2)/Pt(1.6) trilayer are shown as red circles. Four contributions to $1/\tau$: effective Gilbert damping α_{eff}, anisotropy axis distribution $\Delta\theta_H$, anisotropy distribution ΔH_k and two-magnon scattering, are extracted by the fitting of (3). (b) Electric field dependence of the effective damping α_{eff} of the MgO/Co/Pt trilayer.